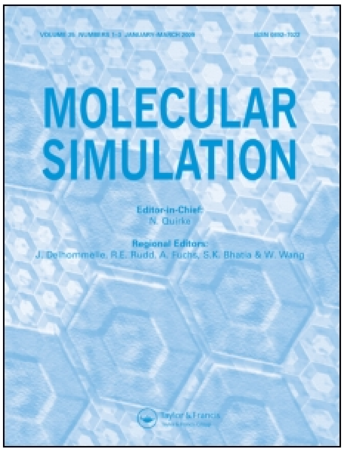

Molecular Simulation
Publication details, including instructions for authors and subscription information:
http://www.informaworld.com/smpp/title~content=t713644482

Classical and Quantum Simulations of Yttrium Cuprate Properties

Roger C. Baetzold[a]
[a] Corporate Research Laboratories, Eastman Kodak Company, Rochester, New York

To cite this Article Baetzold, Roger C.(1994) 'Classical and Quantum Simulations of Yttrium Cuprate Properties', Molecular Simulation, 12: 2, 77 — 87
To link to this Article: DOI: 10.1080/08927029408022525
URL: http://dx.doi.org/10.1080/08927029408022525

Molecular Simulation, 1994, Vol. 12, pp. 77–87
Reprints available directly from the publisher
Photocopying permitted by license only

CLASSICAL AND QUANTUM SIMULATIONS OF YTTRIUM CUPRATE PROPERTIES

ROGER C. BAETZOLD

Corporate Research Laboratories, Eastman Kodak Company, Rochester, New York 14650-2001

(Received February 1993, accepted June 1993)

The defect properties of a number of yttrium cuprate materials have been studied with shell-model and quantum mechanical methods. We find that the structures of $YBa_2Cu_3O_7$, $YBa_2Cu_3O_{6.5}$, and $YBa_2Cu_4O_8$ are reasonably reproduced with a single interatomic potential with deficiencies that are pointed out. Frenkel defects on the oxygen sublattice are the dominant computed defect in those materials. Impurity substitution at particular sites has been studied with a quantum mechanical model. In the case of Ca^{2+} substitution for Y^{3+}, there is a sharp reduction in the ionization potential for formation of delocalized holes in the CuO_2 plane.

KEY WORDS: Yttrium cuprate, Frenkel, Schottky, impurity, shell-model, Hartree-Fock

1 INTRODUCTION

Electronic and ionic point defects are important species in determining the superconducting properties of the cuprate materials. One example concerns the oxygen ion vacancy in $YBa_2Cu_3O_{7-x}$ where $0 \leq x \leq 1$. The superconducting transition temperature (T_c) is a strong function of the oxygen ion vacancy concentration [1, 2]. Since the oxygen ion vacancy concentration is a function of preparation procedures, such as annealing conditions, these defects become important in relating physical properties to environmental conditions. The oxygen ion vacancies are known to occur principally at the O_1 site of the crystal structure shown in Figure 1. There is also evidence [2] of a lower concentration of vacancies on the O_4 site in $YBa_2Cu_3O_{7-x}$.

Another important point defect category in these systems is impurity ions. Numerous impurities substituted on the metal ion site of $YBa_2Cu_3O_{7-x}$ have led to a decrease in T_c, rather than a hoped for increase. Of course, T_c is only one property of interest in these materials. One interesting exception to this trend has involved Ca^{2+} impurities added to the $YBa_2Cu_4O_8$ system, where T_c increases [3] as much as 10 K for impurity levels up to 10%.

The two examples above indicate the importance of defects in the yttrium cuprate materials. The treatment of defects in this system provides substantial challenges for simulation studies. In this paper, we would like to illustrate an aspect of this problem involving the complementary role of classical shell-model calculations within the Mott-Littleton approach [4], and quantum mechanical Hartree-Fock calculations within the Ionic Crystal with Electronic Cluster: Automatic Program (ICECAP) approach [5-8]. We shall study the energetics of vacancy and impurity

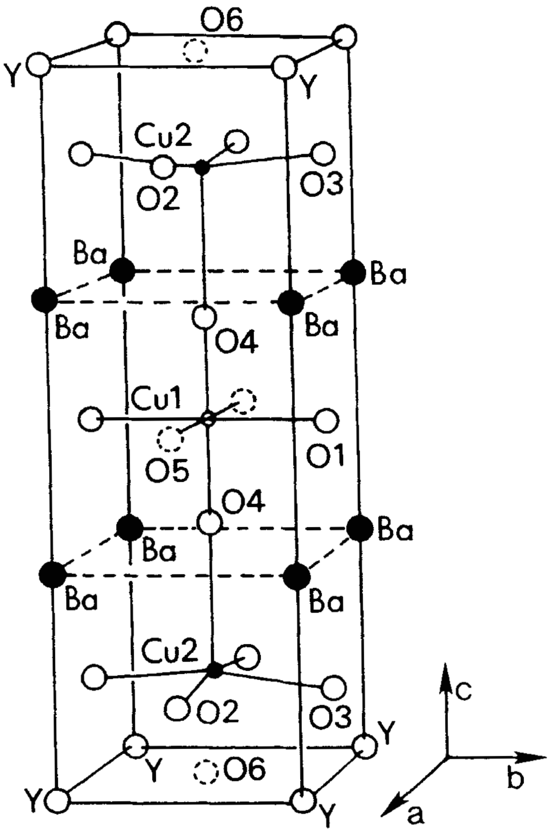

Figure 1 Unit cell of $YBa_2Cu_3O_7$ giving the site designation of oxygen and copper ions.

introduction with the classical methods and electronic features with the quantum methods to illustrate this complementary role.

2 METHOD

The classical methodology that we employ has been described in detail previously [9], where the reader may turn for details. The shell-model calculations treat the interactions between ions using long-range Coulombic terms and short-range N-body terms. Only two-body terms are considered in this work, which uses a Buckingham interaction.

$$\phi(r) = Ae^{-r/\rho} - C/r^6 \tag{1}$$

where A, ρ and c are parameters to be determined. Defects energetics are computed with the Mott-Littleton approach within the framework of the HADES III [10] or CASCADE [11] computer program, allowing full polarization of ions.

The quantum mechanical calculations are of the embedded cluster type using the ICECAP [5–8] methodology. The cluster is treated at the unrestricted Hartree-Fock (UHF) level and coupled self-consistently with the shell-model lattice ions. An initial guess of the charge distribution of the cluster is used to find the positions and polarization of the shell-model ions representing the lattice. The resulting field acts on the cluster ions, which are now computed quantum mechanically. This gives a charge distribution that is expanded in a multipole series and that is used to compare to a similar expansion of the classical representation. Simulator charges are added to the classical distribution to represent the difference and the process is repeated to self-consistency. In practice, we consider up to quadrupole terms in the expansion.

The use of quantum mechanical methods in conjunction with shell-model calculations will be illustrated for yttrium copper oxide clusters containing Ca impurities. The cluster chosen for this study is shown in Figure 2 and contains four yttrium ions, as well as two copper and seven oxygen ions. This is a reasonably large cluster that includes sites for ion substitution, plus ions located in the copper-oxygen plane where electronic effects can be determined. In order to preserve symmetry, we consider substitution, at all four yttrium sites in Figure 2. The $YBa_2Cu_3O_7$ crystal model contains 2 O(1) oxygen ions, while in the $YBa_2Cu_3O_6$ model, these, O(1) ions are missing. We employ Bachelet, Hamann and Schluter (BHS) pseudopotentials [12] for the Y, Ca, and Cu ions with a full basis set for O ions. The basis of the pseudopotential ions are the outer *s* functions for Y^{3+}, optimized from the Huzinaga exponents [13], and the other basis functions have been described before [14]. The appendix contains the exponents and coefficients of the functions we employ.

3 RESULTS

Interatomic potentials have been developed for $YBa_2Cu_3O_{7-x}$ $0 \leqslant x \leqslant 1$ through fitting to the experimental crystal structure [15] of the $x = 0$ member. The starting point for the parameters in these Buckingham type short-range potentials is values from potentials known for other oxides or from electron-gas type of potentials [16]. Our experience has been that additional fitting to the crystal structure is required to obtain a good structure representation. In the case of $YBa_2Cu_3O_7$, a fit of the nearest-neighbor ionic distances to better than 1.5% is achieved. The orthorhombic crystal structure is found when a constant pressure relaxation is performed. The ability to reproduce the low symmetry crystal structure provides a good calibration for the interatomic potentials near the equilibrium distances, but would not guarantee accuracy at significant departures from equilibrium distances. Thus, there remains grounds for refining potentials based upon experimental physical properties or other theoretical methods.

The potential derived above can be applied to predict the crystal structure of other members of the $YBa_2Cu_3O_{7-x}$ series or $YBa_2Cu_4O_8$. Consider the latter crystal. Most of the interatomic distances are fit to better than 1.0%, with the largest discrepancy for the Cu_1-O_4 distance where the error is 3.0%. The orthorhombic crystal structure is found upon "constant pressure" relaxation (in which cell dimensions are varied) but the "a" lattice distance is greater than the b distance by 1.8%, in contradiction to experiment. This error has been corrected by refitting [17], but

Table I Frenkel and Schottky energies per defect

	Potential 1		*Potential 2*	
Crystal	*Frenkel*[a]	*Schottky*[b]	*Frenkel*	*Schottky*
$YBa_2Cu_3O_7$	1.19	4.28	0.77	2.16
$YBa_2Cu_3O_{6.5}$	0.78	4.05	0.76	2.26
$YBa_2Cu_4O_8$	3.00	5.75	–	–

[a] The Frenkel energy for oxygen ions with vacancies at O_1 and interstitials at O_5.
[b] The Schottky defect involving thirteen vacancies is considered.

here we will make comparisons based upon the same potential. Clearly, this is an example of the type of error discussed above when there are deviations from the equilibrium distance of the original compound. Application of the $YBa_2Cu_3O_7$ potential to members such as $YBa_2Cu_3O_{6.5}$ [18] gives a fit of interatomic distances to experiment of better than 2.9%. Thus, overall a single potential with reasonable fit to several members of the yttrium cuprate system can be employed.

The potential described above can be criticized for other reasons. One is that it is known that holes exist in the copper-oxygen planes and the potential in question has only Cu^{2+} and O^{2-} in the plane. Also, there is the matter of the static dielectric constant that is expected to be infinite in the superconducting region. In an attempt to examine some of these points, we derived a second potential [18] for $YBa_2Cu_3O_7$ and $YBa_2Cu_3O_{6.5}$ based upon the experimental hole concentration [19] in the CuO_2 plane of 0.2. We found that the major qualitative trends in terms of ionic and electronic defect energies were not changed in comparing results from the two potentials. Table I shows the Frenkel and Schottky energies for several yttrium cuprates where potential 1 is the same for all [20] and potential 2 has holes in the CuO_2 plane and a larger dielectric constant [18]. Both potentials are specified in the appendix and give a Frenkel defect energy per ion that is smaller than the corresponding Schottky energy. The defect energies are reduced using potential 2 due to its greater screening in terms of the static dielectric constant and presence of holes in the CuO_2 plane. It is interesting that the Frenkel energy of the $YBa_2Cu_4O_8$ compound is larger than that for the other compounds. This feature may be responsible for the greater stability of the compound [21] and the smaller deviations reported from the stoichiometric composition when compared to $YBa_2Cu_3O_{7-x}$.

The Frenkel defects considered above involve oxygen ions at the interstitial site 5 (see Figure 1) and vacancies at site 1 within the CuO chain region. Oxygen vacancy formation energies are compared for the three yttrium cuprates in Table II. For the O_7 compound, the vacancies form most easily at site 1 or site 4 where oxygen vacancies are also detected experimentally [2]. On going to the $O_{6.5}$ compound, the differences between oxygen vacancy formation energy in the chain (O_1 or O_4) versus plane (O_2 or O_3) is decreased, but for potential 1 the vacancies are formed most easily at site 1, as is observed experimentally. For $YBa_2Cu_4O_8$, oxygen vacancy formation has a similar energy at the chain or plane.

The energetic changes on substitution of single impurity ions at various sites in the $YBa_2Cu_3O_7$ crystal have been computed. The impurity-oxide interatomic potentials were taken from previous work [22] in metal oxides systems where empirical potentials were derived. The general result is that trivalent metal ions

Table II Oxygen ion vacancy formation energy (eV)

	Potential 1			*Potential 2*	
Site	$YBa_2Cu_3O_7$	$YBa_2Cu_3O_{6.5}$	$YBa_2Cu_4O_8$	$YBa_2Cu_3O_7$	$YBa_2Cu_3O_{6.5}$
1	17.23	18.50	21.97	18.66	19.97
4	17.34	18.81	20.41	18.31	19.78
2	21.90	21.25	21.79	19.76	19.87
3	21.76	21.51	21.64	19.63	19.91

such as Co^{3+} and Fe^{3+} have an energetic preference to substitute for Cu^{2+} ions in the site 1 and lead to additional oxygen ion incorporation. Divalent metal cations have an energetic preference to substitute for Cu^{2+} ions in site 2 in the CuO_2 plane. Examples from this calculation include Ni^{2+} and Zn^{2+}. Experiments tend to support these calculations with perhaps some exceptions for Zn^{2+} where the situation is quite complex. It is interesting that all of these impurities substituting on Cu^{2+} sites depress T_c in $YBa_2Cu_3O_7$.

The energy of substitution is a smooth function of the ionic radius of the impurity ions. The most favorable energy for substitution is found for impurities with an ionic radius close to that for Cu^{2+}. Of course, impurities can substitute at other sites in the crystal where Ba^{2+} or Y^{3+} ions are located. We examined [23] divalent metal oxide incorporation by the reactions,

$$MO + Cu_{Cu} \rightarrow M_{Cu} + CuO \tag{2}$$

$$MO + Ba_{Ba} \rightarrow M_{Ba} + BaO \tag{3}$$

$$MO + Y_Y \rightarrow M_Y + 1/2\, V_0 + \frac{1}{2} Y_2O_3 \tag{4}$$

where M = Mg, Ca, Sr, Fe, Co, Ni, Zn, and Cd, the subscript denotes the site of substitution and V_0 is an oxygen vacancy. The energy change was always most favorable for reactions (2) or (3) compared to (4).

An interesting impurity effect has been reported in the $YBa_2Cu_4O_8$ system doped with Ca^{2+} [3]. Experiments have shown an increase of T_c of 10 K at a 10% doping level. The suggestion has been advanced that Ca^{2+} substitutes for Y^{3+}, and this adds holes to the system, which increases T_c. Some experiments (24) have contradicted this suggestion, and indicated that the majority of Ca^{2+} substitutes for Ba^{2+} ions. This experiment suggests another mechanism leading to T_c increases must be taking place.

We have computed the energetics of Ca^{2+} substitution in $YBa_2Cu_4O_8$ using potential 1. Various reactions are considered,

$$CaO \rightarrow Ca_Y + 1/2\, V_0 + 1/2\, Y_2O_3 + 3.0\, eV \tag{5}$$

$$CaO + 1/4\, O_2 \rightarrow Ca_Y + 1/2\, Y_2O_3 + Cu^{3+} + 4.8\, eV \tag{6}$$

$$CaO + O^{2-} + 1/4\, O_2 \rightarrow Ca_Y + 1/2\, Y_2O_3 + O^- + 5.1\, eV \tag{7}$$

$$CaO \rightarrow Ca_{Ba} + BaO + 2.5\, eV \tag{8}$$

where V_0 is an oxygen ion vacancy, Ca_x represents the Ca^{2+} at a Y or Ba site

Table III Parameters used to compute reaction energies

Parameter	*Value*
CaO - lattice energy	−36.2 eV
Y_2O_3 - lattice energy	−142.2 eV
BaO - lattice energy	−31.4 eV
Ca_y	27.85 eV
O^-	15.96 eV
Ca_{Ba}	−2.33 eV
Cu^{3+}	−29.69 eV
O_2 - dissociation energy	5.16 eV
O - first electron affinity	1.47 eV
O - second electron affinity	−8.75 eV

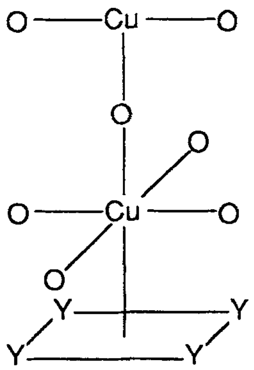

Figure 2 Quantum cluster model $Y_4Cu_2O_7$ used for simulation studies of $YBa_2Cu_3O_7$.

designated by x, Cu^{3+} is a small polaron containing a hole on a copper ion, and O^- is the corresponding small polaron on an oxygen ion site.

The energy change for these reactions is computed from the appropriate lattice energies, vacancy energies, substitution energies, and molecular oxygen dissociation energy and electron affinities. We tabulate these terms in Table III. Each reaction is found to be endothermic, but there is a preference for substitution at Ba^{2+} compared to Y^{3+}. Of course, such a result does not exclude some substitution at the Y^{3+} site, since the energy differences we compute are not large.

We have chosen to investigate Ca^{2+} substitution in yttrium cuprates with quantum mechanical calculations. Such calculations complement the shell-model calculations, and include possible covalent bonding effects. We consider models for $YBa_2Cu_3O_7$ that should give behavior similar to that in the $YBa_2Cu_4O_8$ system. The $Y_4Cu_2O_7$ cluster in Figure 2 is considered. The net charge, Mulliken populations, and ionization potentials calculated for these clusters are given in Table IV. Ionization potentials are computed by the energy differences of the appropriate initial and final charge states.

We begin with the $Y_4Cu_2O_7$ cluster representing undoped $YBa_2Cu_3O_7$. The Mulliken populations correspond quite closely to the formal charges O^{2-} and Cu^{2+}. We do not show populations of the yttrium ion, since these values are less

Table IV Mulliken populations and ionization potentials of $Y_4Cu_2O_7$ model clusters

	Populations					
Cluster	Cu_1	Cu_2	O_1	O_4	$O_{2,3}$	*IP (eV)*
$Y_4Cu_2O_7^{3+}$	9.08	9.06	9.99	9.95	9.99	0.88
$Y_4Cu_2O_7^{4+}$	9.08	8.94	9.96	9.98	9.77	4.33
$Ca_4Cu_2O_7^{-}$	9.09	9.05	9.94	9.98	9.99	−1.82
$Ca_4Cu_2O_7^{0}$	9.09	9.05	9.95	9.98	9.74	0.54
$Y_4Cu_2O_7Ca_4^{11+}$	9.08	9.06	9.99	9.95	9.99	1.52
$Y_4Cu_2O_7Ca_4^{12+}$	9.07	8.94	9.99	9.95	9.76	4.48

Table V Mulliken populations and ionization potential YCu_2O_5 model clusters

	Populations				
Cluster	Cu_1	Cu_2	O_4	$O_{2,3}$	*IP (ev)*
$Y_4Cu_2O_5^{6+}$	10.00	9.06	10.00	9.99	3.35
$Ca_4Cu_2O_5^{2+}$	10.00	9.06	10.00	9.99	−0.43
$Y_4Cu_2O_5Ca_4^{14+}$	10.00	9.06	10.00	9.99	1.75

than 0.001. Ionization of this cluster gives a delocalized hole on the Cu(2) and oxygen ions at sites and O(2) O(3), as has been found in earlier work [14] on similar clusters.

Now consider the $Ca_4Cu_2O_7$ cluster resulting from substitution of Ca^{2+} ions for Y^{3+} ions. We begin with the nominal net charge state that has nearly the same Mulliken population as the Ca^{2+} free cluster. We note that the Ca^{2+} Mulliken population is less than 0.001, as is also true for the Y^{3+} population in the cluster containing these ions. The first and second ionization potentials are sharply lowered by the presence of Ca^{2+}. The change in population upon first ionization indicates that the electron is coming largely from the oxygen ions in the CuO_2 plane. This result is broadly similar to the result found for the cluster with no Ca^{2+} ions. The sharp reduction in first and second ionization potentials clearly indicates it is easier to put holes in the CuO_2 plane when Ca^{2+} ions are substituted for Y^{3+} ions. Such a result would be expected, based upon Coulombic considerations.

Finally, we consider the $Y_4Cu_2O_7$ cluster, in which four shell-model ions representing Ba^{2+} (the rectangular array around O_4) are replaced by Ca^{2+} shell-model ions. In this cluster the Mulliken populations and changes in population are similar to those discussed above. The ionization potentials are slightly increased over the other clusters. This result implies more difficulty in putting holes in the CuO_2 plane when Ba^{2+} ions are replaced by Ca^{2+} ions.

The results of Ca^{2+} substitution have also been examined in models representing $YBa_2Cu_3O_6$ by omitting the two O_1 ions in the cluster shown in Figure 2. The Mulliken populations given in Table V for this $Y_4Cu_2O_5$ cluster are in accord with a Cu^+ ion at the Cu_1 site and a Cu^{2+} ion at the Cu_2 site. Here this result is very consistent with models of the charge distribution invoked for $YBa_2Cu_3O_6$, since the Cu^+ ion has only a twofold oxygen ion coordination. Replacement of Y^{3+} ions by Ca^{2+} again causes a sharp reduction of the ionization potential, indicating that substitution would lead to holes in the CuO_2 plane. The model in which Ba^{2+} ions are substituted by Ca^{2+} shell-model ions has a reduced ionization potential versus the $Y_4Cu_2O_5$ cluster, which should promote hole formation through this type of cluster.

Our quantum mechanical calculations were not used to determine the likelihood of where Ca^{2+} ions will substitute for Y^{3+}, as we determined in the shell-model. Rather, the calculations predict the result that would occur if Ca^{2+} can substitute at a particular site in the crystal. They indicate that for both $YBa_2Cu_3O_7$ and $YBa_2Cu_3O_6$, substitution of Ca^{2+} for Y^{3+} would make it easier to form delocalized holes in the copper-oxygen plane. Based on the known correlations of T_c with hole concentration [25], this result is consistent with the increase in T_c discussed earlier for $YBa_2Cu_4O_8$. Substituting Ca^{2+} for Ba^{2+} does not make it easier to form delocalized holes in the CuO_2 plane. The ionization potential is slightly increased for the $YBa_2Cu_3O_7$ model, and holes are introduced at Cu, for the $YBa_2Cu_3O_6$ models. Thus, the evidence is more complex for Ca^{2+} substitution at Ba^{2+} sites. In addition, there are significant structural changes observed upon Ca^{2+} substitution for Ba^{2+}. A single Ca^{2+} ion is computed to relax 0.68 Å towards the nearest CuO_2 plane when substituted for Ba^{2+} ions, and it is possible that these structural changes do effect T_c.

4 CONCLUSIONS

Shell-model Mott-Littleton calculations and quantum mechanical calculations such as ICECAP play a complementary role in materials simulation studies. We have attempted to illustrate this point in application to the $YBa_2Cu_3O_{7-X}$ system. The shell-model calculations were used to determine ion defect energies. It was found that Frenkel defects on the oxygen sublattice are dominant over Schottky defects in $YBa_2Cu_3O_7$, $YBa_2Cu_3O_{6.5}$, and $YBa_2Cu_4O_8$. The Frenkel energy per defect is considerably smaller in the first two materials as opposed to the latter, which may account for increased stability of $YBa_2Cu_4O_8$ reported experimentally [21]. These results pertaining to ionic defects have been found to be qualitatively the same in calculations using different potentials.

It is difficult to understand how much error might be introduced in various computed properties through the use of purely ionic models. Clearly, metallic properties such as those including screened Coulomb effects [26] are important in these materials. The ionic model reproduces structure well, and it has found successful applications in diffusion studies [27] of ions in these materials. Our previous experience with impurity substitution suggests that a realistic simulation is possible with the method. Our calculations of Ca^{2+} substitution have given support for substitution at the Ba^{2+} site as compared to the Y^{3+} site. This does not preclude possible nonequilibrium effects that may occur in the high temperature preparation of these materials, leading to some Ca^{2+} on Y^{3+} sites.

Our quantum mechanical simulations have given support for a hole delocalized on Cu^{2+} and O^{2-} ions in the plane of $YBa_2Cu_3O_7$, as also found in earlier calculations [14]. These calculations examined the effect of Ca^{2+} substitution on the formation of holes in the CuO_2 plane. It was found that the ionization potential is reduced for the formation of these holes if Ca^{2+} substitutes for Y^{3+}. This effect would be consistent with explanations of the observation of increased T_c of

$YBa_2Cu_4O_8$ with Ca^{2+} doping. On the other hand, the effects of substitution for Ba^{2+} are complex, and a mechanism may operate that leads to T_c increase due to structural changes.

APPENDIX

The parameters of the short-range potential models are given in Table A1. In Table A2 we give the exponents and coefficients of basis sets used in our calculations.

Table A1 Parameters of classical potentials used in this work

	Short-range parameters					
	Potential 1			*Potential 2*		
Interaction	*A (ev)*	$\rho(\text{Å}^{-1})$	$C\ (eV\text{Å}^6)$	*A (eV)*	$\rho(\text{Å}^{-1})$	$C\ (eV\text{Å}^6)$
Cu-O	3799.3	0.24273	0.0	6278.7	0.22262	0.0
Cu-X[a]	6276.0	0.22074	0.0	26783.0	0.18829	0.0
O-O	22764.0	0.1490	75.0	22764.0	0.1490	75.0
O-X	22764.0	0.1490	75.0	22764.0	0.1490	75.0
X-X	22764.0	0.1490	75.0	22764.0	0.1490	75.0
Ba-O	3115.5	0.33583	0.0	32603.5	0.23905	0.0
Ba-X	29194.2	0.24823	0.0	276389.9	0.20566	0.0
Y-O	20717.5	0.24203	0.0	797.4	0.375570	0.0
Ba-Ba	2663.7	0.2588	0.0	-	-	-
Ba-Cu	168128.6	0.22873	0.0	1767512.0	0.21385	0.0

	Shell-model parameters			
	Potential 1		*Potential 2*	
Ion	*Y*	$k(eV/\text{Å}^2)$	*Y*	$k(eV/\text{Å}^2)$
Cu	2.0	999999.0	2.00	999999.0
O	−3.2576	49.8	−3.612912	49.8
X	−3.2576	100.0	−3.2576	100.0
Ba	9.1173	426.1	9.1173	426.1
Y	3.00	999999.0	3.00	999999.0

[a] X designates an O ion at site 1 or 4.

Table A2 Basis sets used in this work

	Oxygen			*Copper*	
Function	*Exponent*	*Coefficient*	*Function*	*Exponent*	*Coefficient*
s1	821.83934	0.01897	d1	45.307828	0.0348034
	123.68182	0.133227		12.636091	0.1757100
	27.66617	0.446412		4.2082300	0.3897658
	7.29957	0.47182		1.3630734	0.4580844
	10.60696	0.052033		0.37550107	0.3141941
	0.91764	0.043176		*yttrium*	

Table A2 *cont.*

Oxygen			*Copper*		
Function	*Exponent*	*Coefficient*	*Function*	*Exponent*	*Coefficient*
	0.28	−0.013178	s1	4.7533447	0.57645125
s2	821.83934	−0.003936		2.129621	0.31045956
	123.68182	−0.029757		0.67786909	−0.94159796
	27.66617	−0.106846		0.28811008	−0.28734391
	7.29957	−0.117476		*calcium*	
	10.60696	−0.074976	s1	5.2942249	0.2185027
	0.91764	0.463203		0.82769456	−0.7201998
	0.28	0.637957		0.34123884	−0.4050154
p2	17.75037	0.034474			
	3.86468	0.190821			
	1.04772	0.370858			
	0.28	0.611384			

References

[1] R.J. Cava, B. Batlogg, C.H. Chen, E.A. Rietman, S.M. Zahurok and D. Werder, "Single phase 60 K bulk superconductor in annealed $Ba_2YCu_3O_{7-\delta}$ with correlated oxygen vacancies," *Phys. Rev. B*, **36**, 5719 (1987).

[2] J.D. Jorgensen, B.W. Veal, A.P. Paulikas, L.J. Nowicki, G.W. Crabtree, H. Claus and W.K. Kwok, "Structural properties of oxygen-deficient $YBa_2Cu_3O_{7-\delta}$, *Phys. Rev. B*, **44**, 1863, (1990).

[3] D.E. Morris, P. Narwankar, A.P.B. Sinha, K. Takano, B. Fayn and V.T. Shum, "Calcium-substituted Y-Ba-Cu-O superconductors with enhanced T_c synthesized at elevated oxygen pressures," *Phys. Rev. B*, **41**, 4118, (1990).

[4] N.F. Mott and M.J. Littleton, "Conduction in polar crystals, I. Electrolytic conduction in solid salts," *Trans, Faraday Soc.*, **34**, 485, (1938).

[5] J. Meng, J.M. Vail, A.M. Stoneham and P. Jena, "Charge-state stability of Ni and Cu impurities in MgO," *Phys. Rev. B*, **42**, 1156, (1990).

[6] R. Pandey and A.B. Kunz, "Simulation of V_K center in LiF using Hartree-Fork clusters," *Phys. Rev. B*, **38**, 10150, (1988).

[7] A.H. Harker, "Quantum-mechanical calculations of defect energies," *J. Chem. Soc., Faraday Trans.*, **85**, 471, (1989).

[8] J.M. Vail, "Theory of electronic defects: Applications to MgO and alkali halides," *J. Phys. Chem. Solids* **51**, 589, (1990).

[9] C.R.A. Catlow and W.C. Mackrodt, in *Computer Simulations of Solids*, Springer-Verlag, West Berlin, FRG, (1982).

[10] M.J. Norgett, Atomic Energy Research Establishment, Harwell, England.

[11] M. Leslie, Science and Engineering Research Council, Daresbury Laboratory, England.

[12] G.B. Bachelet, D.R. Hamann and M. Schluter, "Pseudopotentials that work: From H to Pu," *Phys. Rev. B*, **26**, 4199, (1982).

[13] S. Huzinaga, *Gaussian Basis Sets for Molecular Calculations*, Elsevier, Amsterdam, (1984).

[14] R.C. Baetzold, R. Grimes and C.R.A. Catlow, "Computational study of hole species in models of the superconducters," in preparation.

[15] R. Beech, S. Miraglia, A. Santoro and R.S. Roth, "Neutron study of the crystal structure and vacancy distribution in the superconductor $Ba_2YCu_3O_{9-\delta}$," *Phys. Rev. B*, **35**, 8778, (1987).

[16] R.G. Gordon and Y.S. Kim, "Theory for the forces between closed shell atoms and molecules," *J. Chem. Phys.*, **56**, 3122, (1972).

[17] X. Zhang and C.R.A. Catlow, "Computer simulation study of pressure-induced structural changes in $YBa_2Cu_4O_8$," *Physica C*, **193**, 221, (1992).

[18] R.C. Baetzold, "Computations of point defect energies in $YBa_2Cu_3O_{6.5}$," *Physica C*, **181**, 252, (1991).

[19] R.F. Wood, "Spin polarons, hole filling, and high T_c superconductivity in $YBa_2Cu_3O_7$," *Phys. Rev. Lett.*, **66**, 829, (1991).

[20] R.C. Baetzold, "Atomistic simulation of ionic and electronic defects in $YBa_2Cu_3O_7$," *Phys. Rev. B*, **38**, 11304, (1988).

[21] T. Miyatake, S. Gotoh, N. Koshizuka and S. Tanaka, "T_c increased to 90 K in $YBa_2Cu_4O_8$ by doping," *Nature*, **341**, 41, (1989).

[22] G.V. Lewis and C.R.A. Catlow, "Defect studies of doped and undoped barium titanate using computer simulation techniques," *J. Phys. Chem. Solids*, **47**, 89, (1986).

[23] M.S. Islam and R.C. Baetzold, "Atomistic simulation of dopant substitution in $YBa_2Cu_3O_7$," *Phys. Rev. B*, **40**, 10926, (1989).

[24] I. Mangelschots, M. Mali, J. Roos, H. Zimmermann, D. Brinkmann, S. Rusiecki, J. Karpinski, E. Kaldis and E. Jilek, "Evidence for Ca substitution in $YBa_{2-x}Ca_xCu_4O_{8\pm y}$," *Physica C*, **57**, (1990).

[25] P.F. Miceli, J.M. Tarascon, L.H. Greene, P. Barboux, J.D. Jorgensen, J.J. Rhyne and D.A. Neumann, "Charge tranfer and bond lengths in $YBa_2Cu_{3-x}M_xO_{6+y}$," *Proc. Mater. Res. Soc.*, **156**, 119, (1989).

[26] A.M. Stoneham and L.W. Smith, "Defect phenomena in superconducting oxides and analogous ceramic oxides," *J. Phys. C*, **3**, 225, (1991).

[27] M.S. Islam, "Computer simulation study of oxygen migration in $YBa_2Cu_3O_7$," *Supercond. Sci. Technol.*, **3**, 531, (1990).